February 2007

Selective assembly of nanoparticles on block copolymer by surface modification

Sanjun Niu
University of Nebraska - Lincoln

Ravi F. Saraf
University of Nebraska-Lincoln, rsaraf2@unl.edu

Published in *Nanotechnology* **18** (2007), 125607 (4 pp); doi: 10.1088/0957-4484/18/12/125607

Submitted October 10, 2006; revised January 4, 2007; published online February 21, 2007.

Selective assembly of nanoparticles on block copolymer by surface modification

Sanjun Niu[1] **and Ravi F. Saraf**

Department of Chemical and Biomolecular Engineering, University of Nebraska–Lincoln, Lincoln, NE 68588, USA

[1] Present address: Baxter Healthcare Corporation, Round Lake, IL 60073, USA
Corresponding author email: rsaraf@unlnotes.unl.edu

Abstract
We have developed a method to selectively deposit nanoparticles on the ordered nanoscale elements of PS–PI–PS (polystyrene–polyisoprene–polystyrene) block copolymer film. The process utilizes reactive ion plasma to selectively modify the PS surface with amine groups to electrostatically attract negatively charged Au nanoparticles. In spite of the strong interparticle Coulombic repulsion, the deposition on PS domains is significantly high. It is observed that the deposition at the edges of the domain is particularly high, forming a percolating nanoparticle necklace. The latter may lead to interesting avenues to fabricate electronic devices.

Block copolymers have long been recognized as scaffolds to pattern nanoparticles to construct hybrid structures for various electronic [1], optical [2, 3] and optoelectronic [4] applications. Earlier studies focused on synthesizing nanoparticles selectively on the nanoscopic elements of the block copolymer [5, 6] to obtain ordered structures and fabricate nanodevices, such as nanowires [7]. In other studies, the hierarchical self-assembly of nanoparticles in a nanoparticle–block copolymer mixture was demonstrated where the particles were selectively drawn towards one of the components of the ordered block copolymer morphology [8–10]. Based on the possibility of coupling the thermodynamic ordering of the block copolymer and the selective interaction of nanoparticles with the components of the block copolymer, spontaneous ordering of nanoparticles is theorized [11–13] and experimentally demonstrated [14, 15]. In this paper we describe a method to selectively deposit pre-synthesized nanoparticles on a (preformed) ordered block copolymer surface using a simple approach where one of the nanoscopic polymer domains is selectively functionalized using reactive plasma.

PS–PI–PS tri-block copolymer, supplied by Dexco, was deposited on a Si (silicon) substrate as a thin film by spin-casting a 1% solution in toluene. Spinning speed was 3,000 rpm and spinning time was 30 s. Initial thickness of the film is 26–28 nm as confirmed by ellipsometry. Molecular weights (MW) of the two PS and central PI blocks are 18,000 Daltons each and 64,000 Daltons, respectively. The isoprene block has 92% 1,4 addition. The molecular weight ratio of PS to PI results in cylindrical morphology [16, 17]. The film was processed by the "solvent annealing" procedure [17] and then was baked for 20 min in vacuum at 50 °C. Next, the film was exposed to corona discharge performed in 85% relative humidity air under ambient pressure and temperature for 3 min (moderate etching) or 4 min (deep etching), followed by a thorough rinse with DI (deionized) water. After the film was dried with air flow, it was exposed to 45 W ammonia plasma at a pressure of 580 mTorr for 10 s. Immediately after plasma treatment, the film was immersed into 10 nm Au nanoparticle solution (purchased from BBinternational) for 8–24 h. The Au nanoparticle surface is negatively charged by ClO_4^- groups (as-received). Concentration of the Au nanoparticles is 5.7×10^{12} particles ml^{-1}. Prior to use, the pH of the Au nanoparticle solution was adjusted by addition of diluted HCl solution (pH = 1.5) to a value of ~5. No salt was added. Finally, the film was vigorously washed with DI water and dried in air flow.

In Figure 1, tapping mode atomic force microscope (AFM) images of the film prior to corona treatment (Figure 1(a)), after corona treatment under moderate (Figure 1(b)) and deep etching (Figure 1(c)) are compared. With moderate etching (Figure 1(b)), while the lateral morphology is intact, the height difference between the crest and trough, Δh, is 6 nm, compared

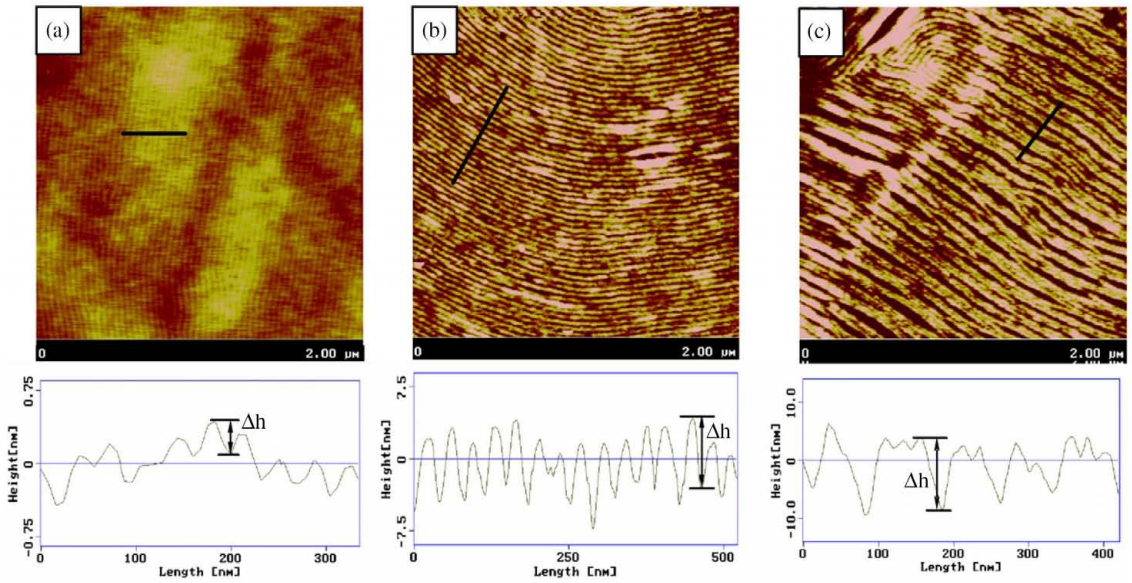

Figure 1. Top view AFM height images and topographic sections of the block copolymer films at three different conditions: (a) as-is, after solvent annealing ($\Delta h \sim 0.3$ nm); (b) after 3 min water vapor corona discharge treatment ($\Delta h \sim 6$ nm); and (c) after 4 min water vapor corona discharge treatment ($\Delta h \sim 14$ nm). Δh shows the average height difference between the crest and trough. The bar on each image indicates the position where the cross section was taken.

with 0.3 nm for the unexposed sample. Since PS is at the crest [17], the increase in Δh due to corona exposure plasma implies that PI which is at the trough is etched at a faster rate. Previous TEM study of the block copolymer has shown that diameters of the PS cylinders were ~14 nm [16]. In Figure 1(c), Δh is 14 nm which is comparable to the diameter of the PS cylinders. Thus it is reasonable to assume that the PS cylinders were not significantly etched and PI was the primary polymer that was etched on corona exposure. Eventually, under deep etching conditions (Figure 1(c)), most of the PI was etched, exposing the underlying Si substrate surface. The cylinders tend to agglomerate when the PI matrix is eroded (observed better in figure 4(b)). Based on the topography measurements from AFM, Figure 2 quantitatively shows Δh as a function of corona exposure time. The nonlinear relationship in Figure 2 is attributed to a change in exposed mass of PI as the etching process progresses. It is known that, in a block copolymer thin film, the low surface energy component covers the entire top of the film. In this case the low surface energy component is PI. Therefore, initially the PI-rich top layer was etched, leading to insignificant change in Δh. As the top layer of PI was etched (at ~2 nm), selective etching occurred and led to higher and nominally constant increase of Δh. We can further note that, although the measured Δh is quantitative for the over-etched sample (Figure 1(c)) where the underlying Si becomes "visible," the measured topographic height for the under-etched sample is less than the actual topography because of the finite shape of the tip that screens the tip from following the surface modulations. Thus, the etch kinetics in Figure 2 is semi-quantitative.

After most of the PI was removed by corona treatment, the surfaces of PS nanocylinders were activated with amine groups by means of NH_3 plasma. To show the hydrophilicity of the PS and PI surfaces after treatment, contact angle tests were performed. The PS surface is more susceptible to NH_3

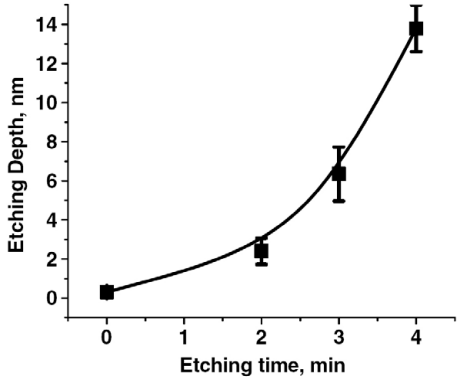

Figure 2. Etching curve of the block copolymer film by water vapor corona discharge. Etching depth is Δh as described in the text. Etching time of zero corresponds to the non-etched film.

plasma than the PI surface. Figure 3 compares water contact angles of homogeneous PS and PI surfaces as a function of exposure time. While the contact angle on the PI surface remains almost unchanged, the PS surface becomes highly wetting due to the formation of amine groups (as confirmed by XPS detection of binding energy of N 1s electrons and by reflection mode FTIR spectrum of H–N–H bond stretching: both were performed on thin block copolymer films after corona and plasma modifications).

The completion of highly selective corona and plasma treatments results in the removal of PI and unsheathed PS nanocylinders with NH_2-rich surfaces. When pH is in the acidic range, the NH_2 groups are protonized so that the PS cylinder surface becomes positively charged. Therefore, upon exposure to the negatively charged Au particle suspension, the particles should deposit selectively on PS cylinders by Coulombic attraction. Figure 4 shows field emission scanning electron microscope (FESEM) images after the deposition

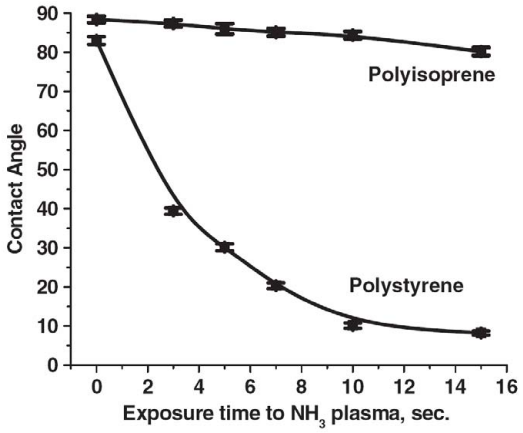

Figure 3. Contact angle comparison as a function of plasma treating time between PS and PI. A treating time of zero indicates no treatment.

of Au nanoparticles. Under both moderate and deep etching conditions, the nanoparticle deposition exhibits a striated morphology that is commensurate with the orientation of the cylinders, confirming the expected strong preference of the negatively charged Au particles for the positively charged PS cylinders. Interestingly, we note that higher deposition occurred at the triple phase line of PS/Si/air (*i.e.,* the edge of the cylinders). The deposition appears to be an electrically conducting (*i.e.,* percolating) one-dimensional necklace of nanoparticles. We discuss a possible explanation in the next paragraph for this new approach to fabricating electronic devices using the electrical property of the nanoparticle necklace structure (see Figure 6).

The high selectivity of Au particle deposition is better observed in a high resolution AFM image by tapping mode for a moderately etched sample (see Figure 5) and in an enlarged view in Figure 4(c). The deposition on the PS cylinders is very high as evident from the nominal width of the two braided nanoparticle rows corresponding to the diameter of a PS nanocylinder. One explanation for such high deposition is charge compensation of the negative charge on the nanoparticle by the positive charge on the highly "aminated" PS chains. The compensation process is expected to be enhanced because of the high mobility of the chains due to surface-influenced mobility, as reported in the literature by noting a significantly lower T_g of surface chains compared to bulk chains [18]. Furthermore, we conjecture, similar to the high density deposition of nanoparticles on bacteria [19], the ~18 kDalton PS chains could wrap around the negatively charged nanoparticles to screen their charges from neighboring particles. The screening will reduce interparticle repulsion, thus leading to the observed high deposition density. The formation of the one-dimensional necklace at the edge of the cylinder may be a combined effect of dipole–dipole interaction between the nanoparticles (that are highly polarizable due to their conductivity) that tend to form linear chains and the edge providing a scaffold to lengthen the chain structure. Such chain-like self-assembly due to dipolar interaction between the nanoparticles has been reported earlier [20].

Electrical conductivity was measured by preparing the Au nanoparticle necklaces on 500 nm thick thermally grown SiO_2 on Si substrates with gold electrodes. The 100 nm thick Au electrodes deposited on the substrate are 7 μm apart. Fig-

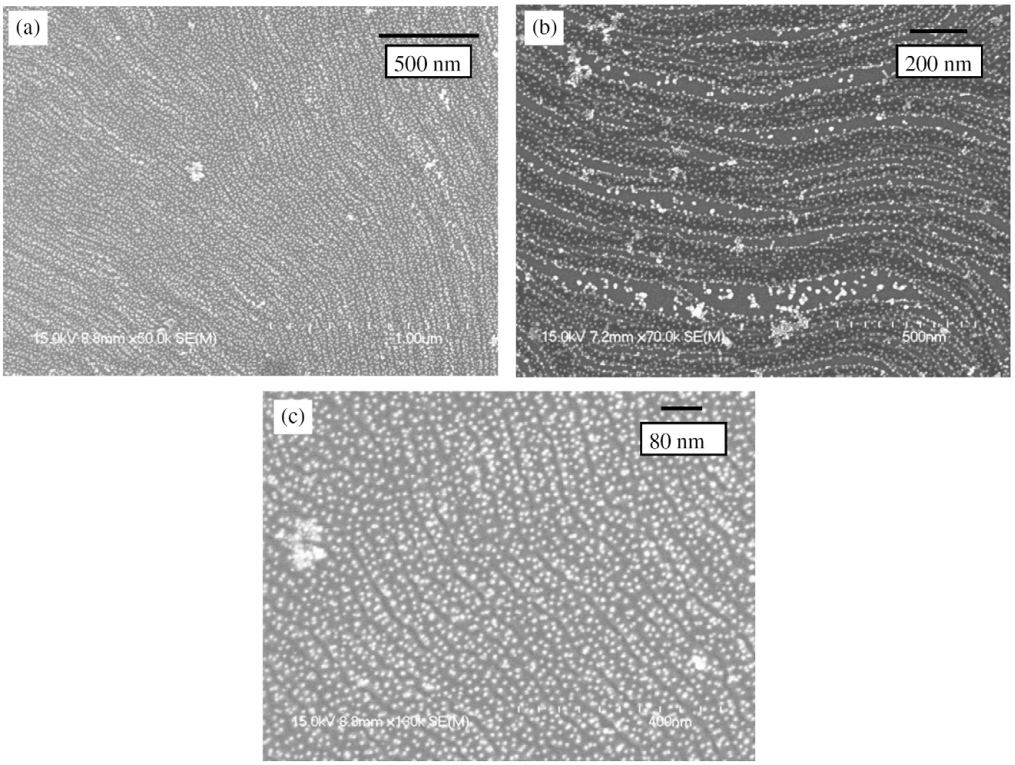

Figure 4. Striated morphology of Au nanoparticles observed by FESEM. The Au nanoparticles deposited on moderately and deeply etched block copolymer films are shown in (a) and (b), respectively. The enlarged view of the center section of (a) is shown in (c).

ure 6 shows the current, I through the network of the necklace as a function of applied bias, V, across the electrodes. The I – V curves were measured at 297 and 5 K at 10^{-6} Torr. The I –V behavior is highly nonlinear and current at 20 V is nominally the same with slightly higher currents at higher temperatures. The insensitivity to temperature indicates that the interparticle transport of electrons is primarily by tunneling, with no significant thermionic transport. Although more conspicuous at 5 K, the I –V characteristics and the differential conductivity characteristics (inset of Figure 6) indicate a typical Coulomb blockade characteristic where the current rises above threshold voltage. A similar behavior of a more resolved blockade effect at lower temperature (compared to room temperature) was observed in a necklace of (nanoscale) metal islands templated on the block copolymer by vapor deposition followed by annealing [8].

The process we developed is quite straightforward and has the potential to be applied to other multiphase systems for selective surface tailoring and deposition. The electrically percolating necklace of nanoparticles could lead to interesting electronic device applications.

Acknowledgment

RFS would like to thank NSF grant CMS-0330227 for financial support.

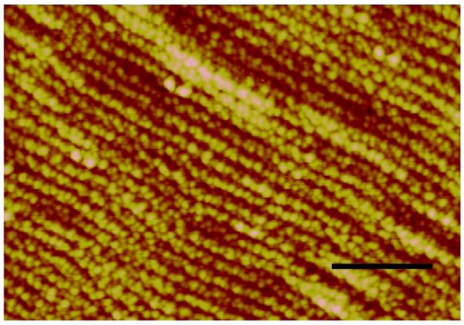

Figure 5. An AFM height image showing high coverage of Au nanoparticles on locally oriented moderately etched block copolymer. The scale bar is 150 nm.

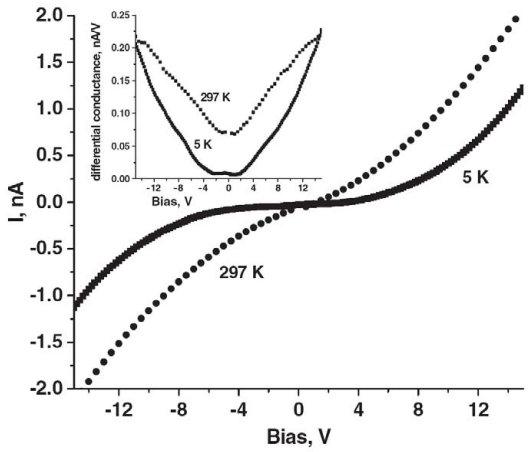

Figure 6. Electrical property of the Au nanoparticle necklace on a deeply etched sample. The main figure shows the I –V characteristics at 297 and 5 K. The inset shows the corresponding differential conductance.

References

[1] Jeoung E *et al* 2001 Fabrication and characterization of nanoelectrode arrays formed via block copolymer self-assembly *Langmuir* **17** 6396–8

[2] Bockstaller M R and Thomas E L 2003 Optical properties of polymer-based photonic nanocomposite materials *J. Phys. Chem.* B **107** 10017–24

[3] Fink Y, Urbas A M, Bawendi M G, Joannopoulos J D, and Thomas E L 1999 Block copolymers as photonic bandgap materials *J. Lightwave Technol.* **17** 1963–9

[4] Li R R *et al* 2000 Dense arrays of ordered GaAs nanostructures by selective area growth on substrates patterned by block copolymer lithography *Appl. Phys. Lett.* **76** 1689–91

[5] Platonova O A *et al* 1997 Cobalt nanoparticles in block copolymer micelles: preparation and properties *Colloid Polym. Sci.* **275** 426–31

[6] Tsutsumi K, Funaki Y, Hirokawa Y, and Hashimoto T 1999 Selective incorporation of palladium nanoparticles into microphase-separated domains of poly(2-vinylpyridine) block-polyisoprene *Langmuir* **15** 5200–3

[7] Peng G W, Qiu F, Ginzburg V V, Jasnow D, and Balazs A C 2000 Forming supramolecular networks from nanoscale rods in binary, phase-separating mixtures *Science* **288** 1802–4

[8] Lopes W A and Jaeger H M 2001 Hierarchical self-assembly of metal nanostructures on diblock copolymer scaffolds *Nature* **414** 735–8

[9] Horiuchi S, Sarwar M I, and Nakao Y 2000 Nanoscale assembly of metal clusters in block copolymer films with vapor of a metal–acetylacetonato complex using a dry process *Adv. Mater.* **12** 1507–11

[10] Lin Y *et al* 2005 Self-directed self-assembly of nanoparticle/copolymer mixtures *Nature* **434** 55–9

[11] Thompson R B, Ginzburg V V, Matsen M W, and Balazs A C 2001 Predicting the mesophases of copolymer–nanoparticle composites *Science* **292** 2469–72

[12] Huh J, Ginzburg V V, and Balazs A C 2000 Thermodynamic behavior of particle/diblock copolymer mixtures: simulation and theory *Macromolecules* **33** 8085–96

[13] Lee J Y, Thompson R B, Jasnow D, and Balazs A C 2002 Effect of nanoscopic particles on the mesophase structure of diblock copolymers *Macromolecules* **35** 4855–8

[14] Bockstaller M R, Lapetnikov Y, Margel S, and Thomas E L 2003 Size-selective organization of enthalpic compatibilized nanocrystals in ternary block copolymer/particle mixtures *J. Am. Chem. Soc.* **125** 5276–7

[15] Chiu J J, Yi G R, Kim B, Kramer E J, and Pine D J 2004 Directed self-assembly of nanoparticles in block copolymer films *Abs. Papers Am. Chem. Soc.* **227** U1451–2

[16] Honeker C C and Thomas E L 2000 Perpendicular deformation of a near-single-crystal triblock copolymer with a cylindrical morphology. 2. TEM *Macromolecules* **33** 9407–17

[17] Niu S J and Saraf R F 2003 Stability of order in solvent-annealed block copolymer thin films *Macromolecules* **36** 2428–40

[18] Wu W L, Vanzanten J H, and Orts W J 1995 Film thickness dependent thermal-expansion in ultrathin poly(methyl methacrylate) films on silicon *Macromolecules* **28** 771–4

[19] Berry V and Saraf R F 2005 Self-assembly of nanoparticles on live bacterium: an avenue to fabricate electronic devices *Angew. Chem. Int. Edn* **44** 6668–73

[20] Tang Z Y, Kotov N A, and Giersig M 2002 Spontaneous organization of single CdTe nanoparticles into luminescent nanowires *Science* **297** 237–40